Fictitious Reference Tuning Using Information in Frequency Domain

Yoshihiro Matsui * **Tomohiko Kimura** ** **Kazushi Nakano** ***

* *Tokyo National College of Technology, 1220-2 Kunugida-machi, Hachioji, Tokyo 193-0997, Japan (e-mail:matsui@tokyo-ct.ac.jp)*
** *Tokyo National College of Technology (e-mail:t-kimura@tokyo-ct.ac.jp)*
*** *The University of Electro-Communications, 1-5-1 Chofugaoka, Chofu, Tokyo 182-8585, Japan (e-mail:nakano@ee.uec.ac.jp)*

Abstract: In this paper, an application method of Fictitious Reference Iterative Tuning (FRIT), which has been developed for controller gain tuning for single-input single-output systems, to state feedback gain tuning for single-input multivariable systems is proposed. Transient response data of a single-input multivariable plant obtained under closed-loop operation is used for model matching by the FRIT in time domain. The data is also used in frequency domain to estimate the stability and to improve the control performance of the closed-loop system with the state feedback gain tuned by the method. The method is applied to a state feedback control system for an inverted pendulum with an inertia rotor and its usefulness is illustrated through experiments.

Keywords: time response, frequency response, stability analysis, disturbance signals, mechanical systems, PID control

1. INTRODUCTION

In recent years, in order to save the time and cost to tune controller parameters for industrial systems, some direct controller parameter tuning methods from the transient response data of the closed-loop systems without modeling the plants have been proposed. Fictitious Reference Iterative Tuning (FRIT) is one of promising candidates for practical direct parameter tuning. See Souma *at el.* [2004] and Masuda *at el.* [2009].

In order to stabilize single-input multivariable systems, state feedback control is often used, and the plant model is necessary to tune the state feedback gain.

In actual state feedback systems, sensors and filters are employed to detect the state variables and to suppress the noises contained in the outputs of the sensors, respectively. Therefore the gains tuned without considering the dynamics of the sensors and the filters do not only achieve desired performance but also may make the closed-loop system unstable. The modeling of the sensors and the filters and the adding them to the plant model prevent the saving of the time and cost to tune the gain.

In this paper, an application of the FRIT to single-input multivariable systems is proposed so that the procedure to tune the gain for state feedback control is easier and less time-consuming. The proposed method is applied to gain tuning for the state feedback control of an inverted pendulum with an inertia rotor. The usefulness of the method is shown through experiments.

The stability of the closed-loop system tuned by the FRIT has been hardly discussed. In this paper, the application of the Nyquist stability criterion to the state feedback control systems tuned by the FRIT is discussed. The improvement of the control performance using the experimental transient data for the FRIT in frequency domain is also shown.

2. STATE FEEDBACK GAIN TUNING BY FRIT

The FRIT is one of model matching techniques to tune controller gain so that the sum of the square error between the output of the closed-loop system with the gain to be tuned and the output of a reference model for the same input during a transient period is minimized. The input for the reference model is called "fictitious reference". The reference is determined so that the input and the output data sets of the plant in the closed-loop system acquired with the initial gain are not varied by the gain change. Therefore any additional experimental data is not required to tune the gain.

To apply the FRIT to state feedback gain tuning, single input multivariable systems are should be seen as Single-Input and Single-Output (SISO) systems. Therefore, in this paper, an n-th order controllable system consists of a system matrix $\boldsymbol{A} \in \mathbb{R}^{n\times n}$, an input matrix $\boldsymbol{b} \in \mathbb{R}^{n\times 1}$, a state feedback gain $\boldsymbol{f}^{\mathrm{T}} \in \mathbb{R}^{1\times n}$ and a unit matrix $\boldsymbol{I} \in \mathbb{R}^{n\times n}$,

$$L(s) = \boldsymbol{f}^{\mathrm{T}}(s\boldsymbol{I} - A)^{-1}\boldsymbol{b}, \tag{1}$$

is seen as a SISO system.

First of all, let's consider the model matching problem shown in Fig. 1. The state feedback gain $\boldsymbol{f}^{\mathrm{T}}$ is tuned so that the sum of square error ε between the output of the actual plant and the output of a reference model $M(s)$ is minimized.

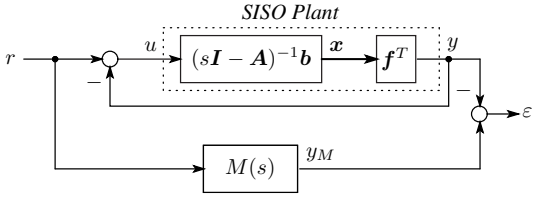

Fig. 1. Model matching problem for single input multivariable systems

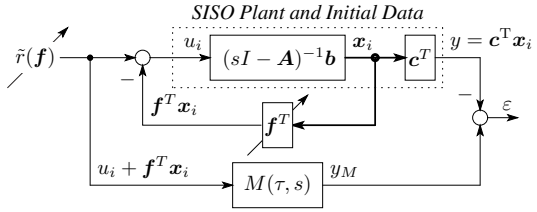

Fig. 2. Modified model matching problem for single input multivariable systems

The problem of the model matching shown in Fig. 1 is that if one of the feedback gains for the state variables is tuned and the other gains are set to zero, the state variable with the feedback gain might be tuned to have almost the same response as that of the reference model and the other state variables are left uncontrolled.

Although all the state variables of the plant are to be tuned in time domain, there is only one loop transfer function to be tuned in frequency domain since the plant is a single-input multivariable system. Therefore, to solve the problem, the model matching problem shown in Fig. 1 is modified as shown in Fig. 2. In Fig. 2 , an output matrix $\boldsymbol{c}^{\mathrm{T}}$ is newly introduced and is tuned in frequency domain so that $\boldsymbol{c}^{\mathrm{T}}(s\boldsymbol{I}-A)^{-1}\boldsymbol{b}$ has good frequency response from the point of view of loop-shaping as mentioned in the next section.

Since the model of the plant and the response speed of the closed-loop system which can be attained by tuning the gain $\boldsymbol{f}^{\mathrm{T}}$ are unknown, the reference model

$$M(\tau,s)=\frac{1}{(\tau s+1)^4} \tag{2}$$

is chosen as the 4th order binomial standard form with a time constant τ to be tuned together with $\boldsymbol{f}^{\mathrm{T}}$. The set of the gain $\boldsymbol{f}^{\mathrm{T}}$ and the time constant τ is defined as

$$\boldsymbol{\rho}=(\boldsymbol{f}^{\mathrm{T}},\tau). \tag{3}$$

The optimal values of $\boldsymbol{\rho}$ given by (4) can be determined to minimize (5).

$$\boldsymbol{\rho}^*=(\boldsymbol{f}^*,\tau^*)=\arg\min_{\boldsymbol{\rho}} J(\boldsymbol{\rho}) \tag{4}$$

$$J(\boldsymbol{\rho})=\sum_{k=0}^{N-1}\varepsilon^2(k)=\sum_{k=0}^{N-1}\{y_M(k)-\boldsymbol{c}^{\mathrm{T}}\boldsymbol{x}_i(k)\}^2, \tag{5}$$

where N is the data length.

In order to avoid iterative experiments to calculate the error ε in (5) for every renewal of ρ to search ρ^*, the fictitious reference defined by (6) is introduced.

$$\tilde{r}(\boldsymbol{f})=u_i+\boldsymbol{f}^{\mathrm{T}}\boldsymbol{x}_i, \tag{6}$$

where u_i and $\boldsymbol{x}_i$ are the transient data sets of the input and the state variables of the plant controlled with a initial stable state feedback gain $\boldsymbol{f}_i^{\mathrm{T}}$ for a reference input r_i, respectively, as shown in Fig.3.

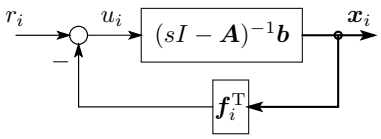

Fig. 3. Data acquisition with initial stable gain $\boldsymbol{f}_i^{\mathrm{T}}$

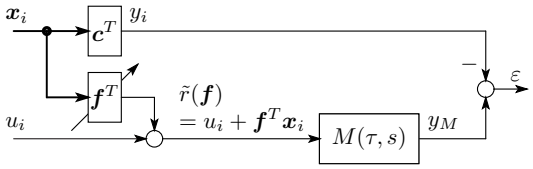

Fig. 4. Equivalent block diagram of Fig. 2

Figure 4, which is the equivalent block diagram of Fig. 2, shows that the error ε can be calculated using only data sets u_i and $\boldsymbol{x}_i$ without any additional experimental data.

The procedure of the search for the optimal values for τ and $\boldsymbol{f}^{\mathrm{T}}$ is as follows: **Step 1**: Acquire the experimental transient data sets u_i and $\boldsymbol{x}_i$ for a reference input r_i, e.g., a step function from the closed-loop system with an initial stable gain $\boldsymbol{f}_i^{\mathrm{T}}$. **Step 2**: Chose a output matrix $\boldsymbol{c}^{\mathrm{T}}$ from the point of view of loop-shaping using the information of u_i and $\boldsymbol{x}_i$ in frequency domain. **Step 3**: Set $\boldsymbol{f}^{\mathrm{T}}=\boldsymbol{c}^{\mathrm{T}}$ in Fig. 4 and obtain τ to minimize (5) by applying bisection method. **Step 4**: Determine $\boldsymbol{f}^{\mathrm{T}}$ to minimize (5) with τ obtained at Step 3 by applying least-square method. **Step 5**: Replace $\boldsymbol{c}^{\mathrm{T}}$ in Fig. 4 with $\boldsymbol{f}^{\mathrm{T}}$ determined at Step 4 and repeat Step 3 and 4 until a terminal condition in terms of the stability of the closed-loop system with the tuned gain is satisfied.

The state feedback gain determined by the procedure is similar to the output matrix $\boldsymbol{c}^{\mathrm{T}}$ and the closed-loop system with the gain is expected to show a good control performance. Therefore the choice of $\boldsymbol{c}^{\mathrm{T}}$ is very important.

3. USE OF INFORMATION IN FREQUENCY DOMAIN

If the gain can be tuned by the data sets u_i and $\boldsymbol{x}_i$ in time domain, the information in frequency domain contained in the data sets is also available. Thus the information in frequency domain is used for the choice of the output matrix $\boldsymbol{c}^{\mathrm{T}}$.

3.1 Estimation of plant frequency response

The frequency response of the transfer function from u_i to $\boldsymbol{x}_i$, that is, $\boldsymbol{P}(s)=(s\boldsymbol{I}-\boldsymbol{A})^{-1}\boldsymbol{b}$ can be estimated (cf.(Matsui *at el.* [2010])) by

$$\hat{\boldsymbol{P}}(j\omega)=\frac{\mathcal{F}_d[\boldsymbol{x}_{if}]}{\mathcal{F}_d[u_{if}]}, \tag{7}$$

where $\mathcal{F}_d$ denotes Discrete Fourier Transform, and $\boldsymbol{x}_{if}$ and u_{if} are filtered $\boldsymbol{x}_i$ and u_i by a filter, respectively. The filter is employed to make $\boldsymbol{x}_i$ and u_i absolutely integrable and to eliminate the discontinuities at the beginnings and the

ends of the sampled $\boldsymbol{x}_i$ and u_i, respectively. The filter used in this paper is a 1st-order high-pass filter given by

$$F(s) = \frac{T_h s}{T_h s + 1}, \tag{8}$$

where the time constant of the filter is given by $T_h = 5T_s$ using the sampling period T_s.

The frequency characteristic of the loop transfer function with an arbitrary gain $\boldsymbol{f}^{\mathrm{T}}$ can be estimated by

$$\hat{L}(j\omega) = \boldsymbol{f}^{\mathrm{T}} \hat{\boldsymbol{P}}(j\omega). \tag{9}$$

3.2 Determination of output matrix

Since $\boldsymbol{f}_i^{\mathrm{T}}$ is a stable gain, $\boldsymbol{f}_i^{\mathrm{T}} \hat{\boldsymbol{P}}(j\omega)$ is the estimated frequency response of a loop transfer function stabilized by $\boldsymbol{f}_i^{\mathrm{T}}$. Therefore, if the features of the frequency response of $\boldsymbol{c}^{\mathrm{T}} \hat{\boldsymbol{P}}(j\omega)$ in terms of the Nyquist stability criterion is the same as those of $\boldsymbol{f}_i^{\mathrm{T}} \hat{\boldsymbol{P}}(j\omega)$, the output matrix $\boldsymbol{c}^{\mathrm{T}}$ is probably a stable gain.

The output matrix $\boldsymbol{c}^{\mathrm{T}}$ should be tuned to keep the above mentioned features in terms of the stability and to have a desirable shape of the frequency response of the loop transfer function with $\boldsymbol{c}^{\mathrm{T}}$ from the view point of loop-shaping, i.e., high loop gain at low-frequencies for steady-state performance, appropriate gain crossover frequency, enough phase margin and continued decrease in magnitude after the crossover.

4. APPLICATION TO INVERTED PENDULUM WITH INERTIA ROTOR

The method explained above is applied to a stabilization control for an inverted pendulum. The inverted pendulum consists of a main cubic body, an inertia rotor and a BLDC motor which drives the inertia rotor as shown in Figs.5 and 6. The BLDC motor is bolted to the square flange which is one of faces of the main cubic body. The pendulum's fulcrum is one of the sides of the cubic body which is orthogonal to the flange surface.

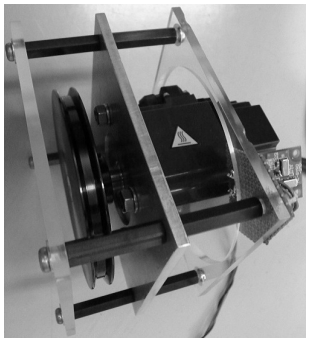

Fig. 5. View of inverted pendulum

The angles θ_1 and θ_2 are the pendulum's tilt from the vertical axis y and the rotation angle of the inertia rotor, respectively. As the state variables defined as $x_1 = \theta_1$, $x_2 = \dot{\theta}_1$, $x_3 = \theta_2$, $x_4 = \dot{\theta}_2$ and the output torque of the BLDC motor u, the linearized state equation of the pendulum is defined by

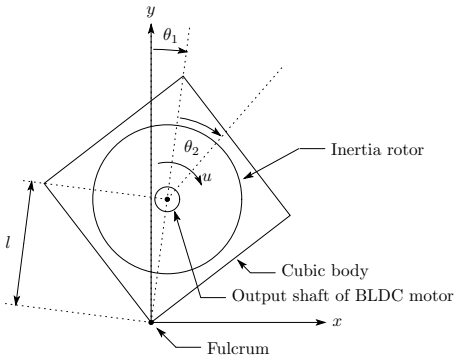

Fig. 6. Model of inverted pendulum

Table 1. Parameters of inverted pendulum

J_1	[kgm^2]	5.44×10^{-3}
J_2	[kgm^2]	7.80×10^{-4}
m	[kg]	2.06
l	[m]	84.9×10^{-3}
g	[kgm/s^2]	9.8

$$\begin{aligned}
\dot{\boldsymbol{x}} &= \boldsymbol{A}\boldsymbol{x} + \boldsymbol{b}u \\
\boldsymbol{A} &= \begin{pmatrix} 0 & 1\ 0\ 0 \\ \dfrac{mgl}{J_1 + ml^2} & 0\ 0\ 0 \\ 0 & 0\ 0\ 1 \\ -\dfrac{mgl}{J_1 + ml^2} & 0\ 0\ 0 \end{pmatrix} \\
\boldsymbol{b}^T &= \left(0, -\frac{1}{J_1 + ml^2}, 0, \frac{J_1 + J_2 + ml^2}{J_2(J_1 + ml^2)}\right) \\
\boldsymbol{x}^T &= (x_1, x_2, x_3, x_4)\,,
\end{aligned} \tag{10}$$

where J_1, J_2, m, l, g are the inertia moments of the cubic body and the rotor, total mass of the pendulum, the length from the fulcrum point to the centroid and the gravity acceleration, respectively. In (10) the viscous resistances are ignored.

The parameters of the pendulum are shown in Table.1.

The transfer functions from the input u to $\boldsymbol{x}$ are given by

$$\begin{aligned}
\boldsymbol{P}(s) &= \begin{pmatrix} P_1(s) \\ P_2(s) \\ P_3(s) \\ P_4(s) \end{pmatrix} \\
&= \frac{1}{(J_1 + ml^2)s^2 - mgl} \\
&\quad \times \begin{pmatrix} -1 \\ -s \\ \dfrac{(J_1 + J_2 + ml^2)s^2 - mgl}{J_2 s^2} \\ \dfrac{(J_1 + J_2 + ml^2)s^2 - mgl}{J_2 s} \end{pmatrix}.
\end{aligned} \tag{11}$$

Since the inverted pendulum is a controllable system, the pendulum can be stabilized at the equilibrium position by state feedback with an appropriate feedback gain given by

$$\boldsymbol{f} = (f_1, f_2, f_3, f_4). \tag{12}$$

4.1 Hardware

Figure 7 shows the hardware of the pendulum. A RISC processor, SH7045 developed by Renesas Technology Corp,

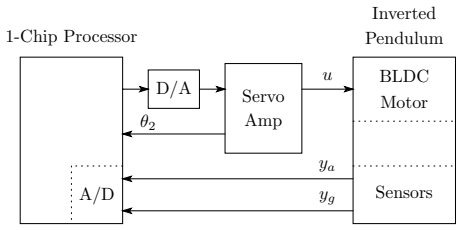

Fig. 7. Hardware for pendulum control

is used as the controller to stabilize the pendulum by state feedback. The sampling period is $T_s = 1$ ms. The processor outputs the torque reference for a servo amplifier which drives the BLDC motor through a DA converter. The rated output power and the rated torque of the BLDC motor are 200 W and 0.637 Nm, respectively.

The detections of the state variables are performed as follows: The pendulum angle, x_1, is detected by the filter with the time constant T_f shown in Fig.8 using the output of a gyroscope sensor y_g and the output of an acceleration sensor y_a. Therefore x_1 is detected by the output of the acceleration sensor and by the integral of the output of the gyroscope sensor at the lower and at the higher frequencies than the angular frequency $1/T_f$, respectively. Therefore the angle of the penculum, x_1 is given by

$$x_1 = \theta_1 = \frac{1}{T_f s + 1} y_a + \frac{T_f s}{T_f s + 1} \frac{1}{s} y_g, \tag{13}$$

where $T_f = 0.5$ s. Thus the detected error of x_1 influenced by the dynamic acceleration which the acceleration sensor outputs and by the integration error generated by integrating the output of the gyroscope sensor is suppressed at the higher and the lower frequencies, respectively. The angular velocity of the pendulum, x_2, is the outputs of the gyroscope sensor filtered by a low pass filter. The angle of the BLDC motor, x_3, is detected by integrating the encoder pulses from the BLDC motor with a counter in the processor. The angle velocity of the BLDC motor, x_4, is detected by the increment of the counter which counts the encoder pulses from the BLDC motor for each sampling period.

As you can see from the above, the sensors and the filters are used for the detections of the state variables in the actual hardware. Since the delays by the AD conversions, the calculation time of the processor and the response time of the servo amplifier in addition the sensors and the filters should be considered, it is difficult to determine the state feedback gain $\boldsymbol{f}^{\mathrm{T}}$ only by the plant model given by (10).

4.2 Acquisition of initial data and estimation of plant frequency response

The initial stable gain for the inverted pendulum determined by trial and error is

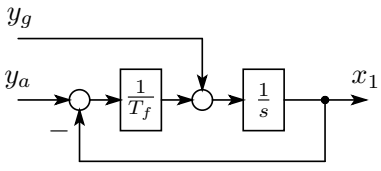

Fig. 8. Estimation of $x_1(=\theta_1)$ with two sensors

$$\boldsymbol{f}_i^{\mathrm{T}} = -(4.54, 0.771, 7.24 \times 10^{-4}, 5.44 \times 10^{-3}).$$

To estimate the frequency responses of $\boldsymbol{P}(s)$ given by (11) , a pulse whose pulse width and amplitude are 50 ms and 1.17 Nm, respectively, is applied to the closed-loop system with $\boldsymbol{f}_i^{\mathrm{T}}$ as a reference input r_i, i.e, a disturbance torque in Fig.3. Figures 9∼12 show the estimated frequency responses of $P_1(s)$, $P_2(s)$, $P_3(s)$ and $P_4(s)$, respectively.

The gains of the estimated frequency responses have peaks at 20 Hz and its harmonics because the amplitudes of the reference input whose pulse width is 50 ms in frequency domain are zero at the frequencies. However it is confirmed that the estimated frequency responses conform with the

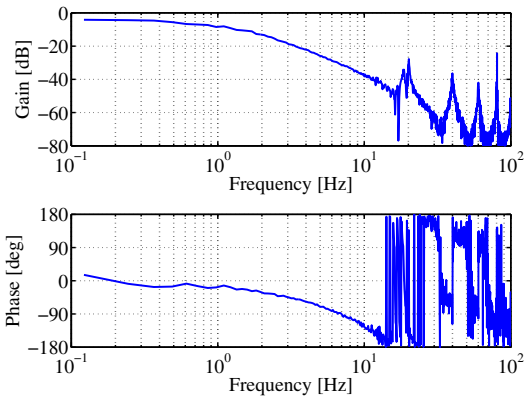

Fig. 9. Bode plot of $\hat{P}_1(j\omega)$

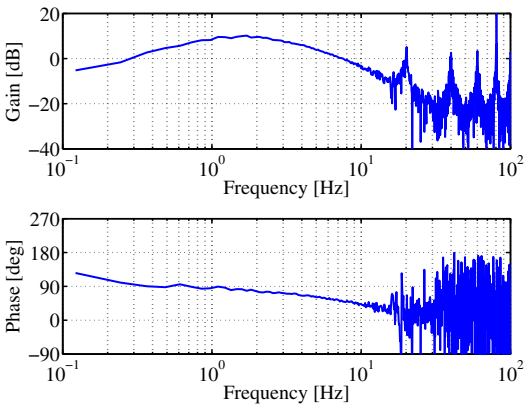

Fig. 10. Bode plot of $\hat{P}_2(j\omega)$

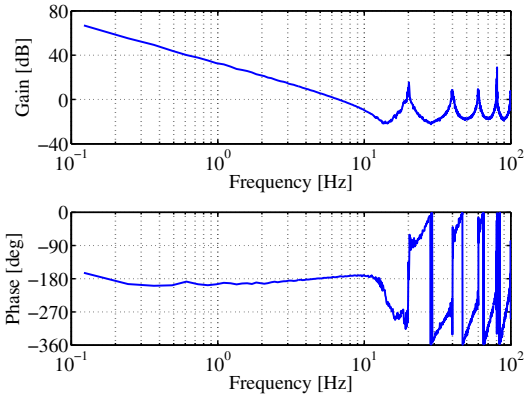

Fig. 11. Bode plot of $\hat{P}_3(j\omega)$

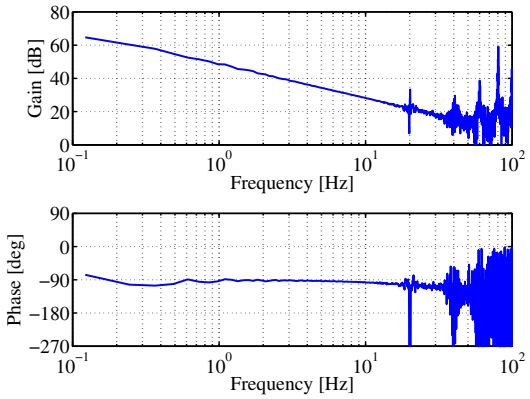

Fig. 12. Bode plot of $\hat{P}_4(j\omega)$

responses given by (11) at the lower frequencies less than about 15 Hz in light of the characteristics of the sensors and the filters to suppress sensor noise.

Figure 13 shows the Bode plot of $\boldsymbol{f}_i^{\mathrm{T}}\hat{\boldsymbol{P}}(j\omega)$ estimated from $\boldsymbol{x}_i$, u_i and $\boldsymbol{f}_i^{\mathrm{T}}$. Although the estimated frequency response at higher frequencies than 20 Hz is not clear because of the noise, the phase and the gain of $\boldsymbol{f}_i^{\mathrm{T}}\boldsymbol{P}(s)$ are -180 deg and less than 0 dB at a higher frequency than 20 Hz because $\boldsymbol{f}_i^{\mathrm{T}}\boldsymbol{P}(s)$ is strictly proper and the phase lag increases as the frequency increases due to the conversion time of AD converter for the sensors and the calculation time of the controller.

The features of $\boldsymbol{f}_i^{\mathrm{T}}\hat{\boldsymbol{P}}(j\omega)$ in terms of the Nyquist stability criterion are as follows: 1) $\boldsymbol{f}_i^{\mathrm{T}}\hat{\boldsymbol{P}}(j\omega)$ has two phase crossover frequencies $\omega_{pcL}/2\pi \simeq 4$ Hz and $\omega_{pcH}(>\omega_{pcL})/2\pi \simeq 30$ Hz in the range of the frequencies shown in Fig.13, 2) $|\boldsymbol{f}_i^{\mathrm{T}}\hat{\boldsymbol{P}}(j\omega_{pcL})| > 1$ and 3) $|\boldsymbol{f}_i^{\mathrm{T}}\hat{\boldsymbol{P}}(j\omega_{pcH})| < 1$.

Since $\boldsymbol{f}_i^{\mathrm{T}}$ is a stable gain, if the state feedback gain tuned by FRIT does not change the features in terms of the Nyquist stability criterion, the closed-loop with the tuned gain by FRIT is probably stable.

4.3 Determination of $\boldsymbol{c}^{\mathrm{T}}$ and gain tuning by FRIT

The loop gain in Fig. 13 is too small at the lower frequencies. Thus it is concerned that the steady-state control performance of the closed-loop system with $\boldsymbol{f}_{\mathrm{I}}$ is relatively poor. In order to amplify the loop gain at the lower

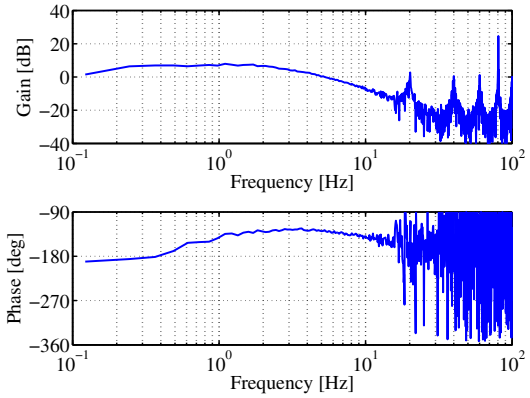

Fig. 13. Bode plot of $\boldsymbol{f}_i^{\mathrm{T}}\hat{\boldsymbol{P}}(j\omega)$

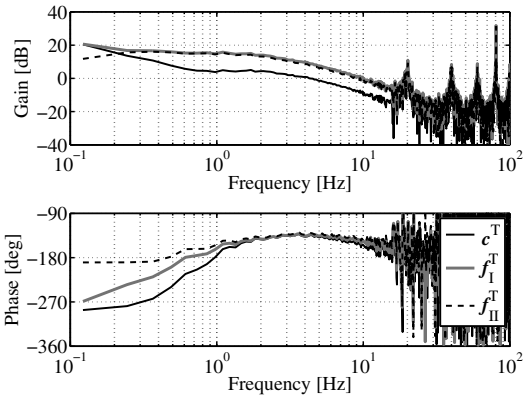

Fig. 14. Bode plots of $\boldsymbol{c}^{\mathrm{T}}\hat{\boldsymbol{P}}(j\omega)$, $\boldsymbol{f}_{\mathrm{I}}^{\mathrm{T}}\hat{\boldsymbol{P}}(j\omega)$ and $\boldsymbol{f}_{\mathrm{II}}^{\mathrm{T}}\hat{\boldsymbol{P}}(j\omega)$

frequencies, the multiplication of the feedback gain for x_3 is effective as Figs.11 shows. And as $x_4 = dx_3/dt$, the multiplication of the feedback gain for x_4 is also important in terms of damping. Therefore the output matrix $\boldsymbol{c}^{\mathrm{T}}$ is determined by

$$\boldsymbol{c}^{\mathrm{T}} = \boldsymbol{f}_i^{\mathrm{T}} \times \mathrm{diag}(1, 1, 5, 10). \tag{14}$$

Figure 14 shows the Bode plot of $\boldsymbol{c}^{\mathrm{T}}\hat{P}(j\omega)$. It also shows the Bode plots of $\boldsymbol{f}_{\mathrm{I}}^{\mathrm{T}}\hat{P}(j\omega)$ and $\boldsymbol{f}_{\mathrm{II}}^{\mathrm{T}}\hat{P}(j\omega)$, where $\boldsymbol{f}_{\mathrm{I}}^{\mathrm{T}}$ and $\boldsymbol{f}_{\mathrm{II}}^{\mathrm{T}}$ are the gains tuned by the proposed method with $\boldsymbol{c}^{\mathrm{T}}$ given by (14) and $\boldsymbol{c}^{\mathrm{T}} = \boldsymbol{f}_i^{\mathrm{T}}$ for comparison, respectively. The gains are

$$\boldsymbol{f}_{\mathrm{I}}^{\mathrm{T}} = -(14.4, 1.94, 4.97 \times 10^{-3}, 6.64 \times 10^{-3}) \textit{ and}$$

$$\boldsymbol{f}_{\mathrm{II}}^{\mathrm{T}} = -(12.6, 1.59, 1.81 \times 10^{-3}, 1.45 \times 10^{-3}).$$

The terminal condition of the procedure of the searches for $\boldsymbol{f}_{\mathrm{I}}^{\mathrm{T}}$ and $\boldsymbol{f}_{\mathrm{II}}^{\mathrm{T}}$ to minimize (5) is that the gain crossover frequency is about 10 Hz because the phase margin for $\boldsymbol{f}_i^{\mathrm{T}}$ is about 40° at 10 Hz as shown in Fig.13.

The Bode plot of $\boldsymbol{c}^{\mathrm{T}}\hat{\boldsymbol{P}}(j\omega)$ has the same features as those of $\boldsymbol{f}_i^{\mathrm{T}}\hat{\boldsymbol{P}}(j\omega)$ in terms of the Nyquist stability criterion and a desirable shape from the view point of loop-shaping as shown in Fig.14.

4.4 Comparison of disturbance responses

The experimental results of the disturbance responses of the closed-loop systems with $\boldsymbol{f}_i^{\mathrm{T}}$, $\boldsymbol{f}_{\mathrm{I}}^{\mathrm{T}}$ and $\boldsymbol{f}_{\mathrm{II}}^{\mathrm{T}}$ are shown in Figs.15 $\sim$ 20. In the figures a pulse whose pulse width and amplitude are 500 ms and 0.466 Nm, respectively, is applied to the pendulum at 10 s as a disturbance torque.

The results show that the low-frequency oscillations of the state variables of the pendulum with $\boldsymbol{f}_i^{\mathrm{T}}$ are improved extremely by $\boldsymbol{f}_{\mathrm{I}}^{\mathrm{T}}$ determined with $\boldsymbol{c}^{\mathrm{T}}$ given by (14).

On the other hand, although the response of $y = \boldsymbol{f}_{\mathrm{II}}^{\mathrm{T}}\boldsymbol{x}$ is well, the responses of the state variables of the closed-loop with $\boldsymbol{f}_{\mathrm{II}}^{\mathrm{T}}$ which was determined with $\boldsymbol{c}^{\mathrm{T}} = \boldsymbol{f}_i^{\mathrm{T}}$ are still undamped as shown in Figs 19 and 20.

The choice of the output matrix $\boldsymbol{c}^{\mathrm{T}}$ to determine the state feedback gain is very important to obtain a good control performance. The choice is possible using the information of the data sets u_i and $\boldsymbol{x}_i$ in frequency domain.

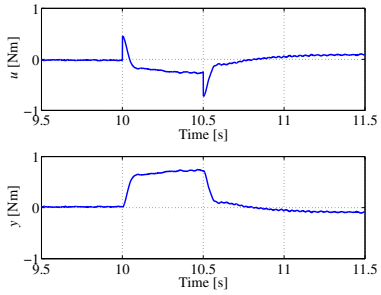

Fig. 15. Responses u and $y = \boldsymbol{f}_i^{\mathrm{T}}\boldsymbol{x}$ of closed-loop system with $\boldsymbol{f}_i^{\mathrm{T}}$

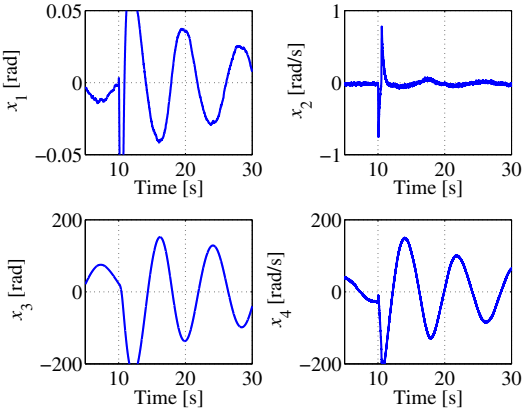

Fig. 16. Responses of state variables of closed-loop system with $\boldsymbol{f}_i^{\mathrm{T}}$

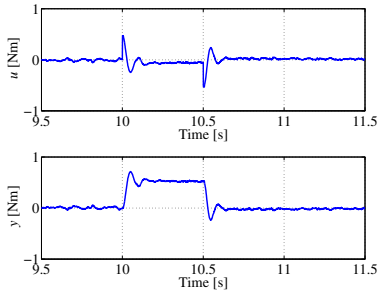

Fig. 17. Responses u and $y = \boldsymbol{f}_{\mathrm{I}}^{\mathrm{T}}\boldsymbol{x}$ of closed-loop system with $\boldsymbol{f}_{\mathrm{I}}^{\mathrm{T}}$

5. CONCLUSION

An application method of the FRIT to the state feedback gain tuning for single-input multivariable systems was proposed. The proposed method was applied to the state feedback gain tuning for an stabilization control of an inverted pendulum with an inertia rotor, and its validity and usefulness were shown through experiments.

REFERENCES

Souma, S., O. Kaneko, T. Fujii (2004). A new method of controller parameter tuning based on input-output data — fictitious reference iterative tuning (frit) —. *Proc. of IFAC Workshop on Adaptation and Learning in Control and Signal Processing*, pages 788–794.

Masuda, S., M. Kano, Y. Yasuda (2009). A fictitious reference iterative tuning meethod with simultaneous delay parameter tuning of the reference model. *International Conf. on Networking, Sensing and Control '09 (ICNSC '09)*, pages 422–427.

Matsui, Y., T. Kimura and K. Nakano (2010). Plant model analysis based on closed-loop step response data. *IEEE Conf. on Control Applications*, pages 677–682.

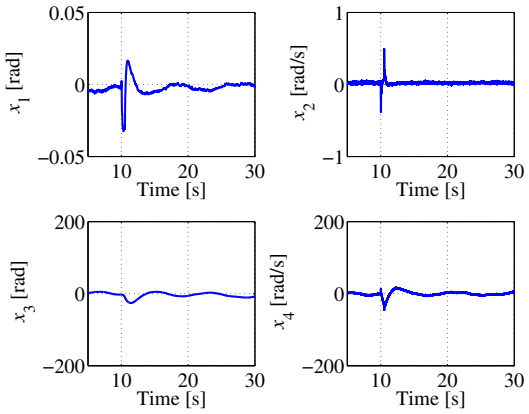

Fig. 18. Responses of state variables of closed-loop system with $\boldsymbol{f}_{\mathrm{I}}^{\mathrm{T}}$

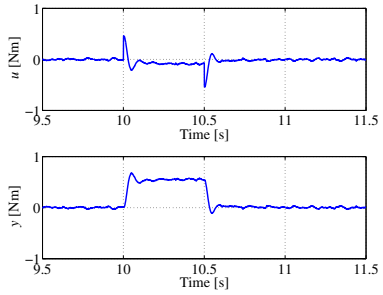

Fig. 19. Responses u and $y = \boldsymbol{f}_{\mathrm{II}}^{\mathrm{T}}\boldsymbol{x}$ of closed-loop system with $\boldsymbol{f}_{\mathrm{II}}^{\mathrm{T}}$

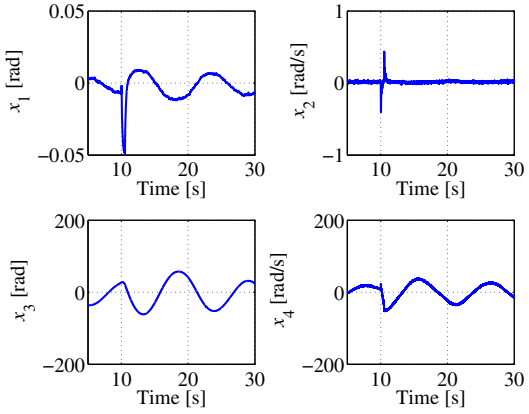

Fig. 20. Responses of state variables of closed-loop system with $\boldsymbol{f}_{\mathrm{II}}^{\mathrm{T}}$